

Pilot-scale Investigation of Heat Flux and Radiation from an Oxy-coal Flame

Andrew Fry¹, Jennifer Spinti, Ignacio Preciado, Oscar Diaz-Ibarra, Eric Eddings
Department of Chemical Engineering and Institute for Clean and Secure Energy, University of Utah

ABSTRACT

The University of Utah is performing ongoing experiments in their 1.5 MW pulverized coal fired furnace (L1500) to better understand the behavior of oxy-coal flames and to provide operating data sets for model validation. In this particular study, the furnace was fired on a Utah Bituminous (Sufco) coal with oxygen and flue gas recycle. A number of experiments were performed throughout a week period, all with identical operating conditions. The multiple sets of data will be used to quantify the repeatability of conditions and the uncertainty in measured values. For these tests the furnace was fitted with 8 water cooled tube bundles in the first four sections of the reactor. The temperature of the water in and out and the temperature of tube surface were measured, along with the cooling water flow rate. A set of three radiometers were installed in the near flame region. These devices were configured to differentiate between radiation from the hot refractory walls and from the coal flame. From these data the heat flux could be determined by multiple methods at four axial locations relative to the flame. Close scrutiny of the heat flux and radiometer data indicate that these techniques are sensitive enough to resolve changes in burner operating conditions. However the magnitude of the heat transfer is not constant throughout a test period due to accumulation of ash on heat transfer and background surfaces.

INTRODUCTION

The Carbon-Capture Multidisciplinary Simulation Center (CCMSC) at the University of Utah is a 5-year US\$16M research program funded by the U.S. Department of Energy through the Predictive Science Academic Alliance Program. The objective of the center is to demonstrate that exascale computing, coupled with formalized Verification & Validation with Uncertainty Quantification (V&V/UQ), can be used to more rapidly deploy new technologies for achieving low cost, low emission, coal-fired power generation. We are using a hierarchical validation approach to obtain simultaneous consistency between a set of selected experiments and simulations at several different scales (0.1 KWth, 100 KWth, 1.5 MWth and 15 MWth) that embody the key physics components (large eddy simulations, multiphase flow, particle combustion and radiation) to predict performance in an industrial-scale facility, which for this project is a 350MWe oxy-fired boiler.

As a portion of the first year activities of this program, oxy-combustion with flue gas recycle (FGR) experiments were performed in the University of Utah's 1.5 MWth pulverized coal furnace (L1500). The furnace was configured with heat flux probes, radiometers and additional temperature measurements. Throughout a week period, operating conditions in the furnace were replicated each day for two burner swirl conditions, thus providing multiple data sets for uncertainty quantification of the data and for validation/uncertainty quantification (V/UQ) of the Large Eddy Simulation (LES) tool that will be used in this program. Key results of the experimentation will be presented here.

¹ Andrew Fry, University of Utah, Research Associate Professor & Director ICGRF, 155 S. 1452 E., Rm. 380, INSCC, Salt Lake City, UT 84112, (801) 587 1781, andrew.fry@utah.edu

EXPERIMENTAL

The L1500 is University of Utah's 1.5 MW pilot-scale pulverized coal furnace and is represented in Figure 1. This furnace has been used for numerous programs investigating NO_x reduction technologies, burner design and flame shape, oxy-combustion [1-3], fuel blending, deposition of mineral matter, corrosion of boiler heat transfer surfaces, SO₃ condensation and emission and mercury control technologies. The overall combustion facility includes the metered air/FGR/O₂ supply system, gravimetric fuel supply system (can be any combination of gas, liquid and solid fuels), burner, water supply and cooling system, radiant section, transition section (radiation barrier), convective section, ductwork, baghouse, scrubber, induced-draft fan and stack.

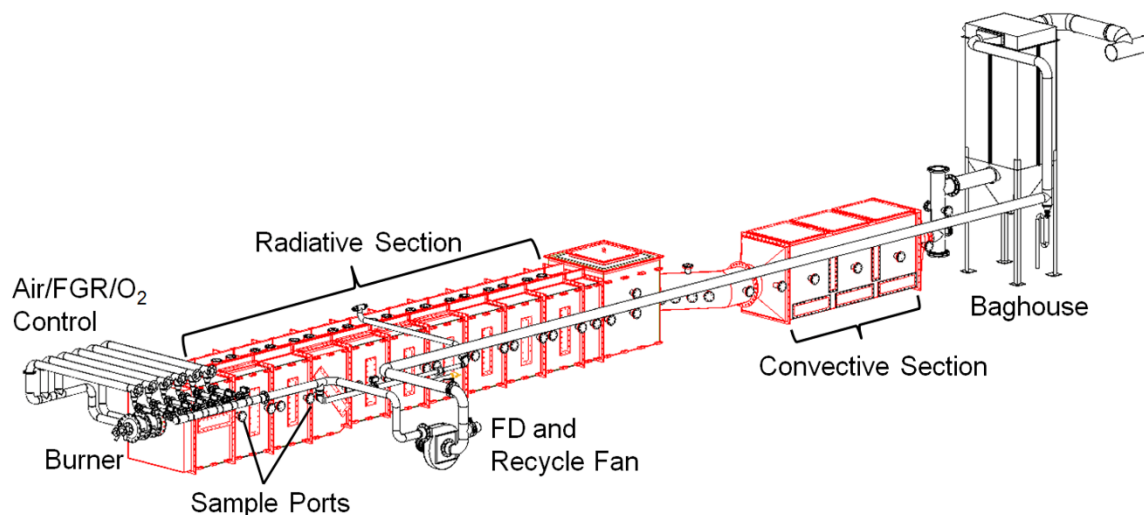


Figure 1. The 1.5 MW pulverized coal combustion test facility at the University of Utah (L1500)

The radiant section of the horizontal-fired combustor is 3.5 ft x 3.5 ft square and nearly 40 ft long. The walls have multiple-layered refractory to reduce the temperature from about 2700 °F on the fire-side to about 300 °F on the outside shell. The combustor is modular in design with numerous access ports throughout and cooling panels in the first four sections. This design allows the flue gas temperature profile to be adjusted to better simulate commercial equipment. The access ports are used for visual observations, fuel and/or air injection, and product sampling.

During the testing, the burner installed on the L1500 was a typical dual register, low-NO_x burner with an IFRF-style adjustable swirl block. The outside diameter of the outer secondary register is 8 inches. The quarl is formed by the refractory wall of the end plate that the burner is mounted on. An additional annulus has been integrated into the burner to provide natural gas to the burner face for furnace heat up and cool down and for maintaining furnace temperature overnight. Details of the low-NO_x burner are presented in Figure 2.

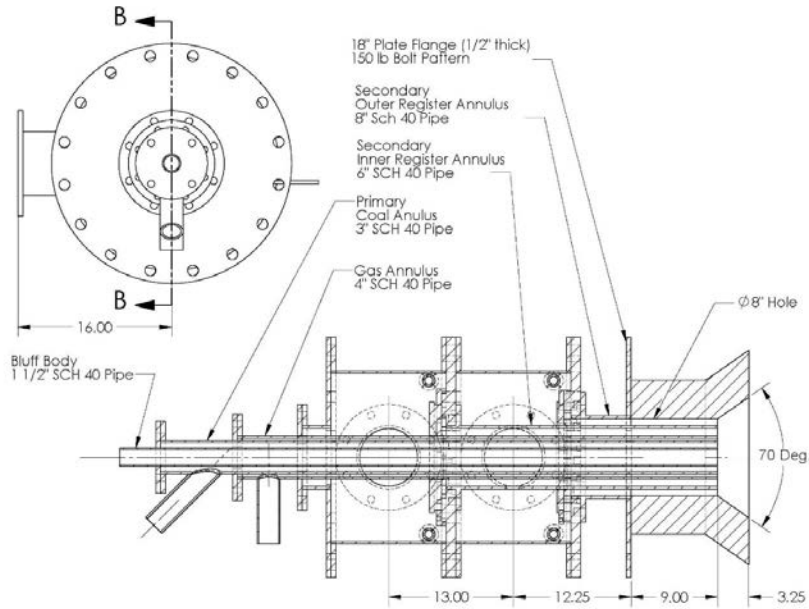


Figure 2. Low-NO_x burner installed on the L1500

Figure 3 provides a scaled representation of the configuration of each of the registers of the burner. The outermost annulus is the outer secondary register and the next is the inner secondary register. Each register can provide air or an O₂/FGR mixture with independent O₂ concentrations and each can operate with different tangential velocities (swirl). The next annulus is for natural gas and is only used to heat the reactor and to keep the reactor warm overnight. The innermost annulus is the coal carrier or primary register. The gas flowing through this register can be either air or an O₂/FGR mixture. In the center of the burner, a bluff body with a range of diameters can be installed to adjust the velocity of the primary gases or to inject oxygen, fuel or reagents. For these tests, the bluff body was not used.

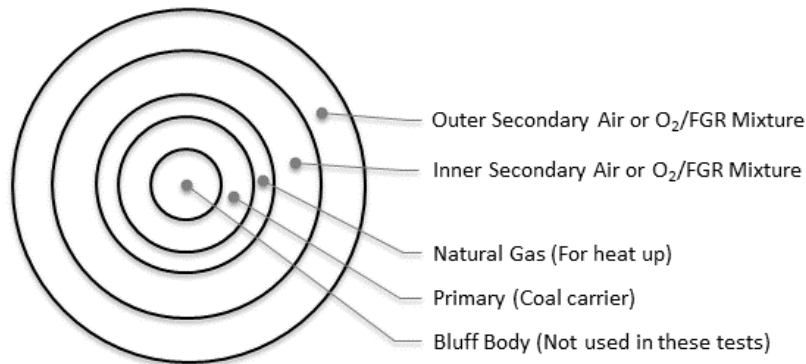


Figure 3. A scaled representation of the registers of the low-NO_x burner

A photograph of the L1500 is included as Figure 4, which includes a view of the air/FGR/O₂ supply system, radiative section and burner.



Figure 4. Photograph of the L1500 depicting the air/FGR/O₂ supply system, burner and radiant section.

The baghouse installed on the furnace is a SLY model SBR-68-8 dust collector. It uses 48 bags of woven fiberglass with Teflon B and PTFE which are 5 $\frac{3}{4}$ " in diameter and 99 $\frac{1}{2}$ " long. For nominal operating conditions at 1.5 MW, the air to cloth ratio of the baghouse is 3 acfm/ft². Cleaning of the bags is accomplished using a pulse jet.

A water-cooled sample probe removes a flue gas sample from the furnace at the inlet to the convective section. This sample is quenched and chilled to remove moisture and is sent to a bank of analyzers whose readings are continuously recorded in the DCS system. The bank of analyzers include: Yokogawa AV8C O₂ (0-25%), California Analytical ZRH CO/CO₂ (0-2000 ppm for CO, 0-20% for CO₂), Thermo Environmental 42C NO_x (0-10,000 ppm) and California Analytical 601 SO₂ (0-5000 ppm).

When oxy-firing with FGR, the flue gas is collected for recycle directly after the baghouse. There is no scrubber or condenser in this line and the SO₂ and moisture contents are somewhat variable depending on the ambient temperatures of the lab and of the equipment. Therefore, the moisture content of the FGR is measured prior to the burner registers.

For these tests, cooling coils were installed in the first four sections of the radiative section on the north and south walls. The coils on the south wall of the furnace are depicted in Figure 5. The cooling media in the coils is water, which is circulated at a high enough rate that steam is not produced. The rate of water flow through each coil is measured in real time along with the temperature in and out of the water. These data are used to determine the total heat removal through each of the eight different coils. Weld-on thermocouples placed on the tube surface of each of the eight coils are used to monitor the tube surface temperature. The thermocouples have a 1" x 1" pad at the tip made of the same stainless material as the cooling coils. The pad is welded over a hole in the cooling coil so that the cooling media makes contact with the pad. The thermocouple wires and sheath are routed internally through the cooling coil to avoid biasing the measurement or complicating the surface geometry of the coils.

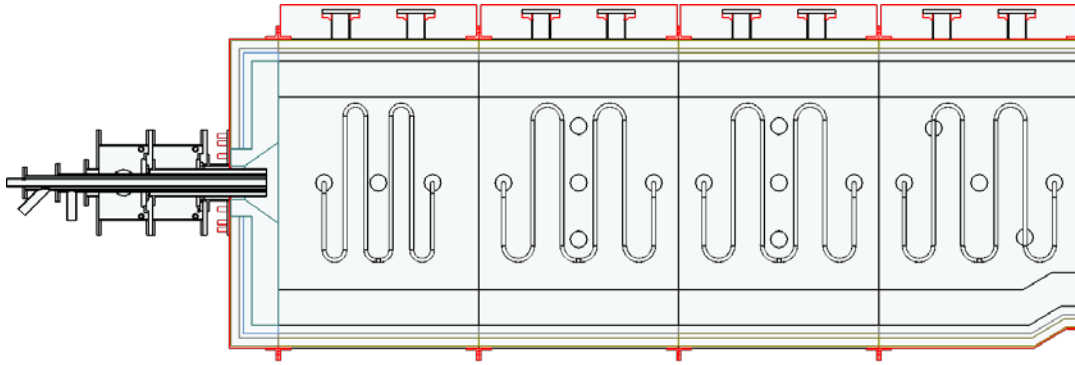


Figure 5. Location of cooling coils in the first four sections of the L1500

Three narrow-angle radiometers were fabricated, calibrated and installed on the south wall of the furnace in the center of the first three sections. A cross-sectional diagram of these probes is presented in Figure 6. The field of view angle for these probes is 2.74 degrees. They are focused on the port holes on the opposite wall of the furnace. In previous testing [1], it was determined that the condition and temperature of the material in the port opposite to these radiometers could significantly influence the measurements. Typically these ports are unused and a refractory blanket wad is installed in them. The surface of the blanket becomes very hot and is highly reflective and the measured heat flux is dominated by the conditions of the opposite wall. For the present tests, a water-cooled plate large enough to encompass the full field of view of the radiometers was installed in the ports opposite the radiometers. These plates also have surface thermocouples welded on. The water temperature in and out and the water flow rate are measured in real time. The resulting data are used to compute heat flux to the wall.

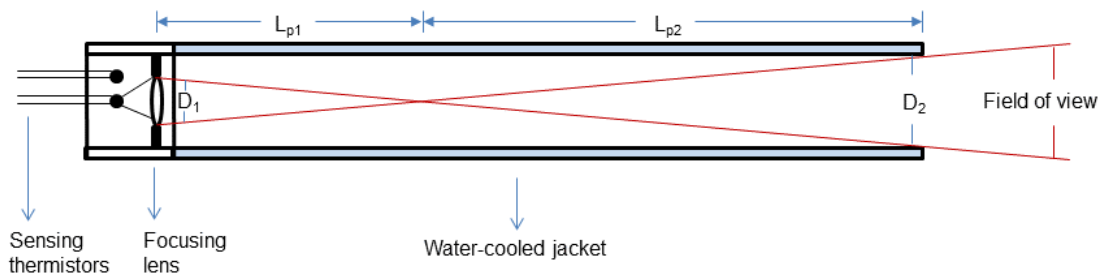


Figure 6. Diagram of the radiometer cross section

Figure 7 is a photograph of one of the narrow angle radiometers. The water flow meter, the purge gas rotameter and the thermocouples can also be seen.



Figure 7. Photograph of narrow angle radiometer

In addition to the cooling coils and the radiometers, ceramic shielded B-type thermocouples were installed in the center of the roof of sections 1-4, 6 and 8. The depth of the thermocouples were adjusted so that the tip of the ceramic shielding was planar with the inside surface of the refractory on the roof. An extractive gas sample probe and sealed sample ports were also prepared so that O₂ and CO concentration profiling could be performed in the center ports of furnace sections 5 through 10.

A Utah bituminous coal from the Sufco mine was chosen for these experiments. Multiple samples of this fuel were collected to determine its composition and particle size distribution (PSD). It was determined that the organic composition of the coal varied little between the samples, but there was appreciable variation of the ash content. The average ultimate and proximate analysis of the multiple coal samples is presented in Table 1.

Table 1. Average Ultimate and Proximate Analysis of Utah Sufco Coal

C	66.9
H	4.5
N	1.2
S	0.4
O	13.6
Ash	7.9
Moisture	5.6
Volatile Matter	40.4
Fixed Carbon	46.1
HHV, Btu/lb	11,765

The PSD was determined using two different methodologies: sieving and laser diffraction. For the sieving method, the sample was placed at the top of the sieve tray stack and the stack was shaken for a set time (15, 20, and 30 minutes). The mass of sample on each tray was then recorded. Repeat tests were run with a few of the samples. For the laser diffraction data, small samples were analyzed using a Beckman Coulter

LS 230. Each sample was run three times and the results were reported in % differential volume.

The PSD data from all samples using both techniques are plotted in Figure 7b. Although not apparent from the figure, the data indicate that the uncertainty in the repeatability of any PSD measurement is as large as the bag-to-bag PSD uncertainty. There are large differences in the data from the 15-, 20- and 30-minute sieving times and there is not yet proof of convergence. Thus, longer times should be tried in the future. Also included in Figure 8 is a Rosin Rammler fit of the 30-minute sieving. To obtain the “true distribution” used in the simulations, the 15- and 20-minute sieving data were rejected because they do not exhibit a Rosin Rammler distribution at the lower end of their particle size range. The remaining 30-minute sieving and laser diffraction data were then fit to a Rosin-Rammler distribution.

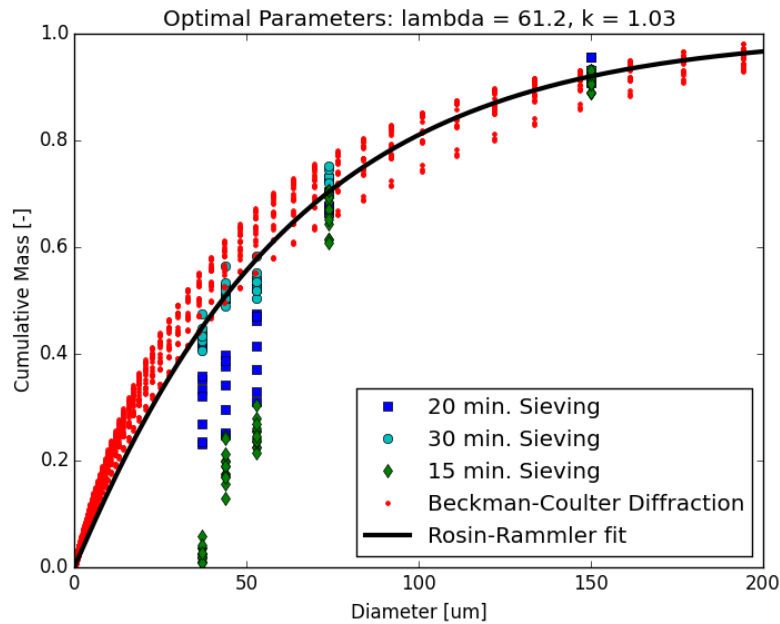


Figure 7b. PSDs obtained by sieving and laser diffraction analysis. The 30-minutes sieving data is fit to a Rosin-Rammler distribution.

EXPERIMENTAL RESULTS

The conditions for furnace operation were chosen to be consistent with the way a retrofitted, coal-fired utility boiler would likely run. The FGR rate was set to provide an overall O_2 concentration in the O_2 /FGR mixture of 27%, wet. This condition provides radiative and convective heat transfer characteristics similar to an air-fired condition, depending on the specific boiler configuration [5-6]. The primary gas to fuel mass ratio was set at 1.8 and the O_2 concentration in the primary register was 21%, wet. The mass split of gas between the inner and outer secondary registers was 20%/80%. The burner operated unstaged (e.g. without over-fire air) and the stoichiometric ratio was set to provide 3% O_2 , dry in the exit flue gas.

Table 2 provides a summary of target gas flows and temperatures that were obtained through material balance calculations for the desired conditions. Table 2 also provides average measured values for each

of the flows when running with 0 and 100 % swirl in the secondary registers. Outlet dry O₂ and CO₂ measurements are also presented. The two swirl conditions have been summarized because of their prominence in the resulting data and because there is feedback from the swirl setting to the achievable conditions in the furnace. There is a discrepancy between the target and actual outlet CO₂ concentrations and the difference changes with swirl setting. This is a representation of air in-leakage which occurs almost exclusively in the recycle fan. The air-leakage is minimized when the backpressure on the fan is minimized. Because of the swirl block configuration of the low-NO_x burner, the 0% swirl condition results in a higher back pressure and thus more air in-leakage.

Table 2. Targeted and Actual Experimental Conditions

	Units	Target	0% Swirl	100% Swirl
Firing Rate	Btu/hr	3.5		
Coal Rate	lb/hr	297.0	297.0	296.9
Primary FGR	lb/hr	450.2	461.9	461.7
Primary O₂	lb/hr	85.3	86.4	86.3
Inner Secondary FGR	lb/hr	361.9	362.0	362.0
Inner Secondary O₂	lb/hr	105.9	114.0	106.3
Inner Secondary Temp	°F	500.0	496.2	502.3
Outer Secondary FGR	lb/hr	1448.6	1440.3	1449.2
Outer Secondary O₂	lb/hr	422.6	418.2	418.4
Outer Secondary Temp	°F	500.0	498.6	501.9
Outlet O₂	%, dry	3.0	2.6	2.9
Outlet CO₂	%, dry	96.1	85.7	88.2

One of the most prominent aspects of the collected data is the amount of heat removal through the cooling coils. These values, along with wall temperature measurements and the heat fluxes measured by the radiometers, will be crucial in the comparing the experimental and simulated thermal environments. Figure 8 provides a snapshot of the heat removal through the cooling coils during a change from 0 to 100% swirl.

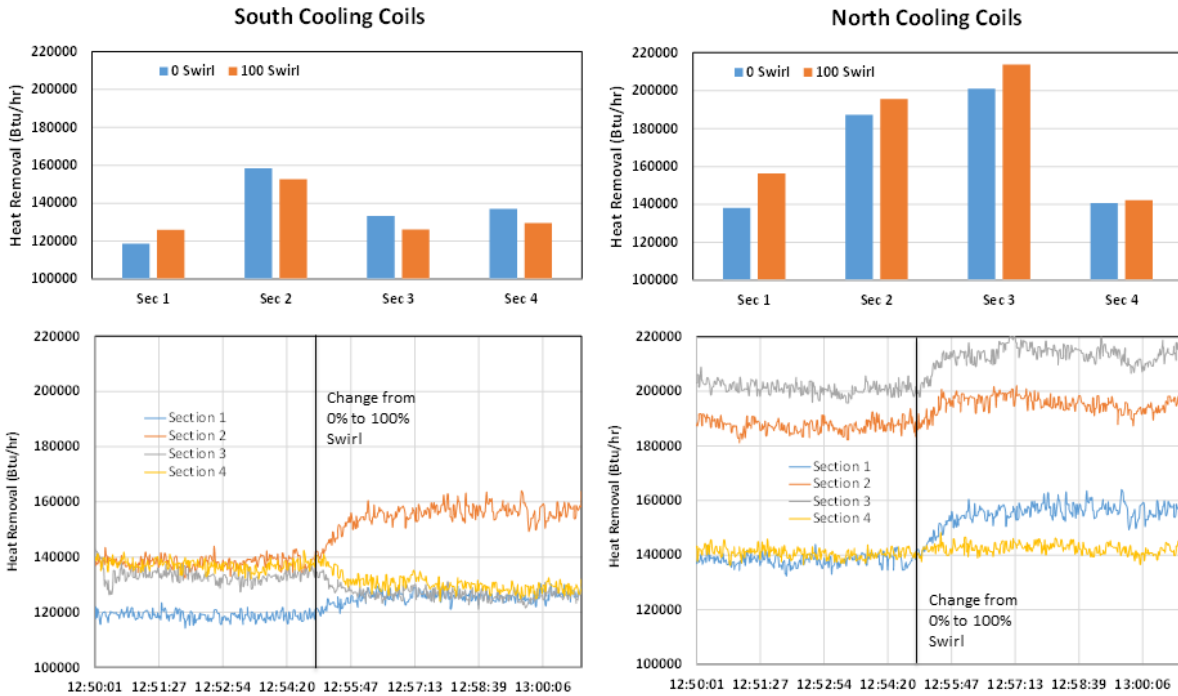


Figure 8. Heat removal through cooling tubes as the burner inner and outer register swirl is changed from 0 to 100% (short time period)

The heat removal data in Figure 8 indicate that coils and their metering provide a rapid response and are sensitive enough to determine the impact of changing burner swirl from 0 to 100%. The observed change in heat distribution matches the expectation that near-burner mixing is increased in the 100% case, resulting in a shorter, more intensely radiating flame. As a result, the heat removal in sections 1 and 2 on the south wall and 1, 2 and 3 on the north wall all increase while the heat removal by the remaining downstream coils decreases.

When these heat flux data are evaluated across long periods of time, it is obvious that the heat removal is decreasing steadily. This phenomenon is presented in Figure 9, which shows heat flux data for more than six hours of operation. Evaluating the heat removal data across several days of operation, including the first day with new clean tubes, it is obvious that the decrease in heat removal is due to continuous buildup of ash on the cooling coils. The ash layer both insulates the tubes and changes the radiative properties of the tube surface. This phenomenon must be considered when using the data for V/UQ analysis.

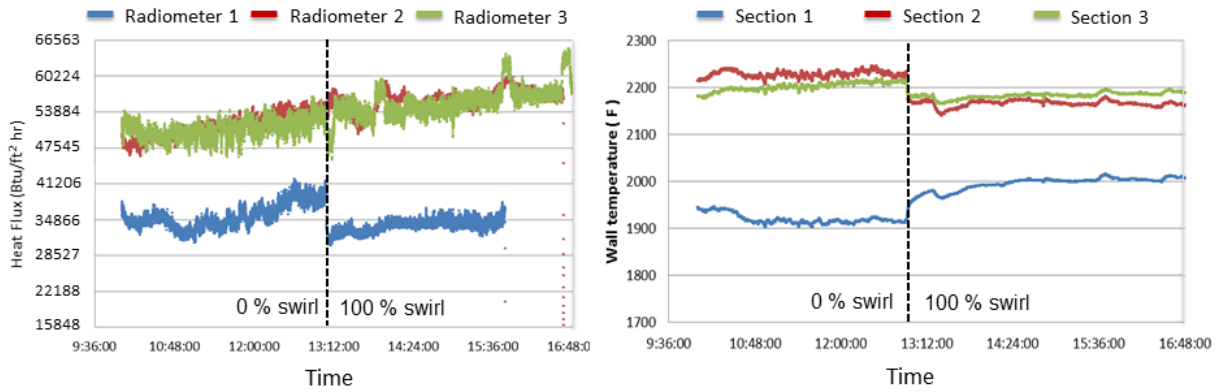


Figure 9. Heat removal through cooling tubes as the burner inner and outer register swirl is changed from 0 to 100% (long time period)

The data in Figure 9 show that the change in heat flux distribution that occurs due to a change in swirl condition is still significant compared to the downward drift of heat removal throughout the day. However, it is difficult to assign a magnitude of experimental heat removal to each of the surfaces when the measured value is constantly decreasing.

The radiometer data for the same period of operation along with the measured wall temperature for the first three furnace sections are presented in Figure 10. These data show that the radiative heat flux is also responsive to a change in burner swirl conditions. Here the radiative heat flux in section 1 decreases as the swirl increases. These data also show that the radiative heat flux in the first four sections increases continuously throughout the period of operation. These radiometers are configured to see a water-cooled plate in the opposite port. During one period of testing when the radiometers were removed from the furnace, it was observed that the water-cooled plate had developed a coating of ash that appeared to be highly reflective. As a result, rather than seeing a cold surface at the opposite wall, the radiometer sees a bright, radiating surface that contributes to the overall heat flux measured. As this buildup increases, the measured radiative heat flux also increases as it includes not only gas radiation but also wall radiation. The lower heat flux observed for radiometer 1 is most likely due to the optical thickness of the dense particle jet exiting the burner which effectively blocks radiation from the opposite wall. It is possible that the narrow field of view for radiometer 1 was partially observing the cooled plate when the swirl was set at zero and when the swirl was increased the field of view was dominated by unburned and burning fuel.

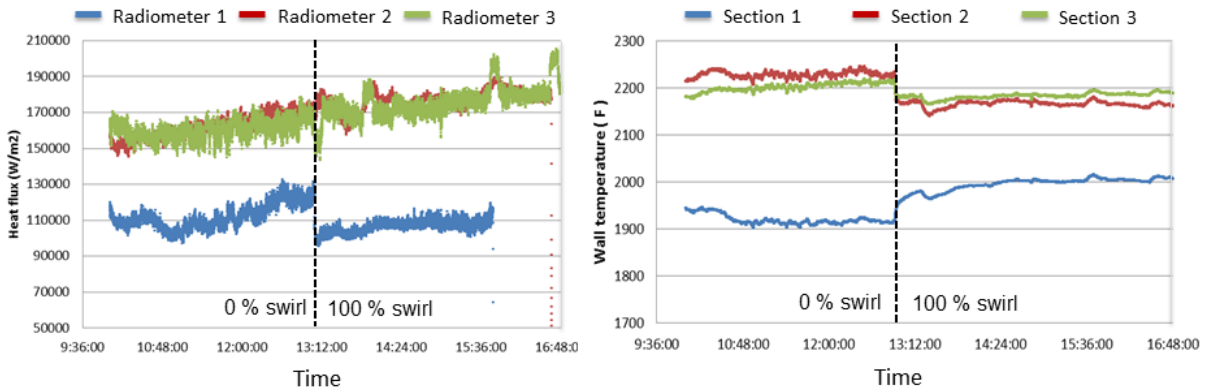


Figure 10. Radiometer data as the burner inner and outer register swirl is changed from 0 to 100% (long time period)

SUMMARY AND CONCLUSIONS

Oxy-combustion tests were performed in a 1.5 MW pulverized coal furnace for the purpose of developing data sets suitable for V/UQ analysis LES modeling. The furnace was fired with a Utah bituminous coal using conditions that are expected to provide similar radiative and convective heat transfer to air-fired combustion in existing utility boilers. Data quantifying the heat removal through cooling coils and the radiative heat flux in the first four sections of the furnace were collected. These data showed a measurable and expected response to a burner swirl change with greater heat release in the near-burner region when swirl was increased from 0 to 100%. However, the magnitude of the heat removal through the cooling coils continuously decreased throughout the testing period. This behavior is indicative of mineral matter deposition on the cooling coil surfaces. The radiometer data shows the opposite trend with increasing radiative heat flux throughout the testing period. A water cooled plate installed on the opposite side of the furnace to the radiometer was supposed to provide a cold surface boundary condition for measuring heat flux due to gas radiation. However, it was observed during testing that mineral matter deposits collected on these plates, resulting in a highly reflective boundary condition on the opposite wall. Thus, as ash built up, the radiometer measurement included not only gas radiation but also radiation from the opposite walls, and the heat flux measured by the radiometers increased accordingly.

These experiments have possibly identified the crux of using pilot-scale data sets for V/UQ analysis of CFD models. A steady-state quantifiable rate of heat transfer through the cooling coils needs to be measured for a given set of conditions. In future testing campaigns focused on the development of validation data sets, a robust method of soot blowing will be considered. This may provide a pseudo steady state condition for heat transfer and also remove much of the interference of the opposite wall for the radiometer measurements.

In addition, detailed information is necessary concerning the physical conditions of the deposit and the deposit metal interface in order to apply the correct emissivity and conductivity characteristics to those surfaces in the model.

ACKNOWLEDGMENTS

This material is based upon work supported by the Department of Energy under Award Number DE-NA0002375.

This report was prepared as an account of work sponsored by an agency of the United States Government. Neither the United States Government nor any agency thereof, nor any of their employees, makes any warranty, express or implied, or assumes any legal liability or responsibility for the accuracy, completeness, or usefulness of any information, apparatus, product, or process disclosed, or represents that its use would not infringe privately owned rights. Reference herein to any specific commercial product, process, or service by trade name, trademark, manufacturer, or otherwise does not necessarily constitute or imply its endorsement, recommendation, or favoring by the United States Government or any agency thereof. The views and opinions of authors expressed herein do not necessarily state or reflect those of the United States Government or any agency thereof.

REFERENCES

1. A. Fry, et. al., Principles for Retrofitting Coal Burners for Oxy-Combustion. *Int. J. Greenh. Gas Con.* **2011**, 55, S151-S158.
2. A. Fry, et. al., An Investigation Into the Likely Impact of Oxy-Coal Retrofit on Fire-side Corrosion Behavior in Utility Boilers. *Int. J. Greenh. Gas Con.* **2011**, 55, S179-S185.
3. J. Ahn, Ryan Okerlund, A. Fry and E.G. Eddings, "Sulfur Trioxide Formation During Oxy-Coal Combustion," *Int. J. of Greenh. Gas Con.* **2011**, 55, S127-S135.
4. Wall, T. F., et al., 2009. An overview of oxyfuel coal combustion – state of the art research and technology development. *Chem. Eng. Res. Des.* 87, 1003-1016.
5. A. Fry, B. Adams, B. Van Otten, "Assessment of Full-scale Boiler Oxy-combustion Retrofit Using CFD Modeling," presented at the IEA Oxyfuel Combustion Conference, Yepoon, Australia, Sept. 13-15, 2011.